Universal teleportation via continuous-variable graph states

Lijie Ren, Guangqiang He,* and Guihua Zeng
State Key Laboratory of Advanced Optical Communication Systems and Networks, Department of Electronic Engineering, Shanghai Jiao Tong University, Shanghai 200240, China
(Received 23 April 2008; published 6 October 2008)

We present a universal protocol for continuous-variable graph-state teleportation. A mathematical model is established to determine an arbitrary graph state's properties, including the possibility of teleportation and the relevant analytical criteria. By investigating the properties of several fundamental graph-state types, we identify a general strategy for optimizing excess noise due to finite squeezing. As an application, a general scheme for teleportation between two arbitrary parties on a two-dimensional square lattice cluster state is given, along with a cheaper yet equivalent optimization for fixed source-target teleportation. Finally, a universal way to distill bipartite entanglement from a graph-state entanglement network is presented based on the equivalence between teleportation and entanglement distillation.

DOI: 10.1103/PhysRevA.78.042302 PACS number(s): 03.67.Hk, 03.67.Lx

I. INTRODUCTION

Quantum teleportation is one of the fundamental operations in quantum communication and computation. The concept of teleportation is that with the assistance of quantum entanglement between two parties one of them can use a classical channel to transmit arbitrary quantum states to the other [1]. Continuous-variable (CV) teleportation [2,3] generalizes the concept of teleportation to continuous degrees of freedom by the use of quadratures, "position" $\hat{x}=\hat{a}+\hat{a}^{\dagger}$ and "momentum" $\hat{p}=-i(\hat{a}-\hat{a}^{\dagger})$.

A major problem in teleportation is the excess noise caused by an imperfect entanglement network due to finite squeezing. One aim of experimentalists is to reduce the excess noise of one or both quadratures in the final mode. When the original mode is a Gaussian state, using the fidelity criterion defined as $F\equiv\langle\alpha_1|\hat{\rho}_{\mathrm{tel}}|\alpha_1\rangle$ [4], we can examine the similarity between the reconstructed mode and the original one. Lower excess noise leads to higher fidelity [5].

In teleportation where only two-mode entanglement is used, higher fidelity is reached only with a higher squeezing level. However, in teleportation where multimode entanglement is employed, there is another factor which has a powerful control on the excess noise and therefore affects the fidelity—the configuration of the entanglement. Teleportation via Greenberger-Horne-Zeilinger-like states has been investigated in [6], with the conclusion that more modes in an entanglement network lead to lower teleportation quality. In the case of graph states, it is the graph itself that has a powerful control on the excess noise. Since each graph state has its own teleportation properties, the situation for graph-state teleportation becomes more complex yet flexible and may have more power for future use. By designing different graphs, one may achieve various results with different costs.

Previous research based on teleportation via graph states was mainly focused on one-dimensional graph types, while the true power of graph-state teleportation lies in the higher-dimensional senarios. In [7], two-dimensional graph states are considered necessary in CV quantum computation to enable multimode gates. However, an exact implementation and error analysis are not given there. In [8] the author suggests a common approach to teleporting quantum information via higher-dimensional graph states by using a disconnection operation, reducing the problem to a one-dimensional one. Such a reduction is easy, yet cannot exploit the advantage the original graph states have in teleportation. In [9] teleportation using multiple-rail encoding based on two-dimensional graph states is demonstrated, showing a possible advantage of higher-dimensional graph-state teleportation. However, these results are rather preliminary and lack generality. In this paper, we generalize the graph to an arbitrary type and investigate its properties under a universal teleportation protocol. Compared with the scheme of linear (i.e., one-dimensional) graph-state teleportation, our protocol can achieve better fidelity in two- and multidimensional graph-state teleportation.

Practical teleportation is usually established on entanglement that has already been prepared. Two types of teleportation between one sender and one receiver among a set of parties are discussed in this paper. One is arbitrary source-target teleportation in which the sender and the receiver are chosen randomly from the set. This kind of teleportation requires an integrated entanglement network which enables any two parties in the set to communicate with each other. The other type is fixed source-target teleportation. The teleportation network between them can be customized to more efficient ones with (perhaps) fewer resources and better fidelity.

In evaluation of a certain graph state's performance in teleporting quantum information, the concept of both cost and benefit is employed in this paper. States prepared with fewer squeezing and coupling resources {i.e., smaller single-mode squeezing factor r, fewer edges [denoting a quantum nondemolition (QND) interaction] in the graph representation of the state, and smaller gains of the QND interaction g (implying less coupling time)} are considered to be cheaper. And final results with less excess noise in one or both quadratures (or simply higher fidelity, in cases where the original state is Gaussian and the excess noise for a single quadrature is of little interest) are considered to be better.

*gqhe@sjtu.edu.cn

Another related problem is entanglement distillation on CV graph states. Since the essential resource for teleportation is bipartite entanglement, the investigation we make on teleportation can be directly translated to that on bipartite entanglement distillation, only with the source mode unmeasured—so we will not break the entanglement between it and the target mode. Thus, by solving the problem of how to teleport via graph states, we simultaneously obtain a method to distill the states to bipartite entanglement.

The plan of this paper is as follows. First, in Sec. II, we propose a universal protocol which can be used in teleportation via arbitrary graph states along with the analysis of related criteria. In Sec. III, some interesting and useful teleportation properties of typical graph states are discussed, which can be used to control excess noise. In Sec. IV, an application to square lattice cluster-state teleportation is given, with less excess noise compared with a one-dimensional scheme. In Sec. V, entanglement distillation on CV graph states is discussed. It is outside the pure region of teleportation yet we think it is worthwhile to mention some preliminary yet interesting conclusions.

II. PROTOCOL OF TELEPORTATION VIA GRAPH STATES

A graph state is generated by coupling a set of zero-momentum eigenstates ($\hat{p}=0$) by QND interaction characterized by the Hamiltonian $H_{ij}=\hbar\chi_{ij}\hat{x}_i\hat{x}_j$. QND coupling between mode i and mode j transforms $\hat{x}_i$, $\hat{p}_i$, $\hat{x}_j$, and $\hat{p}_j$ in the Heisenberg picture to the following expressions [8]:

$$\hat{x}_i' = \hat{x}_i, \quad \hat{p}_i' = \hat{p}_i + g_{ij}\hat{x}_j,$$

$$\hat{x}_j' = \hat{x}_j, \quad \hat{p}_j' = \hat{p}_j + g_{ji}\hat{x}_i, \tag{1}$$

where $g_{ij}=g_{ji}=-\chi_{ij}t_{ij}$ is the gain of the interaction between the ith and jth modes. χ_{ij} and t_{ij} are the coupling coefficient and the interaction time, respectively.

Thus, a general graph state of N modes can be described in the Heisenberg picture by

$$\hat{x}_i^g = \hat{x}_i, \quad \hat{p}_i^g = \hat{p}_i + \sum_{j=1}^{N} g_{ij}\hat{x}_j, \quad i = 1,2,\ldots,N, \tag{2}$$

where

$$g_{ij} = g_{ji} = \begin{cases} -\chi_{ij}t_{ij}, & j \in N_i, \\ 0, & j \notin N_i, \end{cases}$$

and the modes $j \in N_i$ are the nearest neighbors of mode i. Here $\hat{x}_i=e^{+r_i}\hat{x}_i^{(0)}$ and $\hat{p}_i=e^{-r_i}\hat{p}_i^{(0)}$ are the two quadratures after squeezing, with r the squeezing parameter and (0) the superscript denoting the initial vacuum modes. For a large r, the $\hat{x}$ quadrature becomes very noisy after squeezing while the $\hat{p}$ quadrature becomes very certain. $r\to\infty$ corresponds to the ideal case of infinite squeezing.

In the following we first recall and clarify two important types of operation on CV graph states and then present the protocol itself along with more detailed explanations and remarks.

A. Two inequivalent ways to distill CV graph states

In CV graph-state distillation, two types of operation are of major importance [8]. One is disconnection based on the concept of undoing the coupling—measuring the $\hat{x}$ quadrature of the mode to be discarded and then displacing the $\hat{p}$'s of all its neighbors by the product of the result and the corresponding gain of the interaction g, which is the exact inverse transformation of the QND interaction described in Eq. (1). Such an operation simply projects the original N-partite entanglement into an $(N-1)$-partite one. The mode that has been measured is discarded without a trace, as if it has never been coupled with the rest of the entanglement (ignoring quantization error due to the finite precision in measuring $\hat{x}$ and g).

The other operation also reduces the original N-partite entanglement to an $(N-1)$-partite one, yet its effect on the preserved entanglement differs from that of disconnection. The concept of this type of distillation operation is given in [7]—if an infinite squeezed mode a with $\hat{p}_a=0$ is coupled with only one mode b, after measuring $\hat{p}_b$ and performing $F^\dagger X(-p_b)$ on mode a with $F^\dagger$ the inverse Fourier transform operator acting as $\hat{x}\to\hat{p}$ and $\hat{p}\to-\hat{x}$ and $X(s)$ the position-translation operator such that, as $\hat{x}\to\hat{x}+s$, mode a becomes the same as the original mode b. If mode b was coupled with another mode c before the measurement, after these operations, the original entanglement chain is distilled to one where modes a and c are coupled directly. Compared with the disconnection operation, this kind of distillation creates new entanglement (in the example above, the entanglement between modes a and c) in the process of destroying the old ones (in the example above, the entanglement between modes a and b and also the entanglement between modes b and c). More importantly, the limited single-mode squeezing degree r of the mode being measured (mode b in the example) has an effect on the final quality of the entanglement after distillation is performed (in the example, the noise of $\hat{p}_b$ is transferred to the noise of $\hat{p}_a$ after the distillation). We use the word "melting" to denote this kind of distillation because of the interesting similarity between the $\hat{p}$ variance of the mode to be discarded and the sugar in a sugar cube to be dissolved in hot water—their forms are lost, but their content is preserved in the environment. When distillation is obtained via the melting operation, a finite squeezing degree may have negative effects on the quality of the distilled entanglement. And that is the reason why teleportation on a one-dimensional graph state with more modes (with the same squeezing degree r) has lower fidelity.

In higher-dimensional scenarios, the melting operation has more complex rules to follow. Previous work [8] suggests that for distillation of a higher-dimensional graph state to bipartite entanglement, we first use the disconnection operation to select a one-dimensional chain which connects the two parties, and then distill the bipartite entanglement from the chain via the melting operation. In the following sections, by investigating teleportation via arbitrary graph states, we actually obtain a universal method to distill a bipartite entanglement from a multidimensional graph state using only (or with less help from the disconnection operation) the melting operation. Unlike in one-dimensional graph states, in

higher-dimensional scenarios, entanglement among more modes does not inevitably lead to worse final bipartite entanglement quality. Thus we find the conclusion inspiring.

B. Universal protocol of graph-state teleportation

Assuming a graph-state entanglement network among several parties (including the sender and the receiver) has been prepared before teleporting, a general teleportation could be realized by performing the following four steps.

(i) Disconnect a subgraph from the original graph state. The subgraph must contain the target mode (i.e., the mode in which we wish to reconstruct the quantum information after teleportation) and at least one mode accessible to the sender. As we will show in the later part of this section, this step is not mandatory and may be skipped sometimes.

(ii) Couple the source mode (i.e., the mode containing the quantum information we wish to teleport) with one or more modes the sender has in the graph state obtained in (i) through a QND interaction, forming a complete entanglement network—the core graph.

(iii) Measure $\hat{p}_i^g$ of all modes in the core graph except the target mode, obtaining outcomes p_i^g.

(iv) Apply a series of $T(s_k)=F^{\dagger}X(-s_k)$ to the target mode. The parameters $s_k=\Sigma_{i=1}^{N-1}c_{ki}p_i^g$ and c_{ki} are graph-dependent coefficients.

We now explain the protocol in more detail. Step (i) is necessary to keep the integrity of the protocol in two respects. One is in practical implementation because the graph state may be so large and complicated that it can enable multiple teleporting tasks. It would be extremely wasteful to use the whole network in only one teleportation. The other is that as we will show in the next section, theoretically, not all teleportation via graph states can be performed purely with steps (ii)–(iv); teleportation via some graph states is realizable only if step (i) is allowed. Step (ii) establishes the entanglement between the source mode and the rest of the teleportation network, which is the precondition for teleportation. Note that, generally, the source mode can be coupled with more than one mode already in the graph state; thus the strategy that first projects the auxiliary entanglement network to a bipartite entanglement and then couples the source mode with one mode in bipartite entanglement is a special case of this protocol. Since after step (ii) the whole state is still a graph state (in a generalized sense in which the original source mode does not have to be an infinitely squeezed one), it is convenient to consider the whole core graph state as one containing the source mode from the beginning and thus omit the coupling operation in step (ii). In the following we will always assume the source mode to be one mode in the original teleportation network. Once the core graph has been prepared, steps (iii) and (iv) (i.e., the melting type of distillation mentioned in Sec. II A) will be adequate to carry out the teleportation. Obviously, the final state is affected only by the core graph—disconnection does not affect the quality of entanglement. Therefore, it is important to study the core graph's teleportation properties under a protocol that is purely composed of steps (iii) and (iv). Under the complete protocol, if there is more than one subgraph that could be chosen as the core graph, we can then choose the most suitable one to meet the teleportation requirement.

In the following, we introduce a general approach to determine whether a graph state can be used as a core graph [i.e., teleportation via the state could be performed purely with steps (iii) and (iv)]. To simplify the following discussion, let us assume the graph state as an N-mode multipartite entanglement network with the source mode indexed 1 and the target mode indexed N. The quantum information to be teleported is the quadratures of mode 1 before coupling (i.e., $\hat{x}_1$ and $\hat{p}_1$).

For a given graph state, let G denote the adjacency matrix with $G_{ij}=g_{ij}$. Using $\hat{R}=(\hat{x}_1\cdots\hat{x}_N|\hat{p}_1\cdots\hat{p}_N)$, Eq. (2) can be rewritten as

$$\hat{x}_i^g=\hat{R}\begin{pmatrix}I_i\\0\end{pmatrix},\quad \hat{p}_i^g=\hat{R}\begin{pmatrix}G_i\\I_i\end{pmatrix},\quad i=1,2,\ldots,N, \tag{3}$$

where G_i is the ith column of G and I_i is the ith column of the identity matrix I.

Performing step (iv) will change mode N from $(\hat{x}_N^g,\hat{p}_N^g)$ into one of the four types

$$\begin{aligned}
&\text{(I)}\quad \hat{x}_{\text{tel}}=u+\hat{x}_N^g,\quad \hat{p}_{\text{tel}}=v+\hat{p}_N^g,\\
&\text{(II)}\quad \hat{x}_{\text{tel}}=v+\hat{p}_N^g,\quad \hat{p}_{\text{tel}}=u-\hat{x}_N^g,\\
&\text{(III)}\quad \hat{x}_{\text{tel}}=u-\hat{x}_N^g,\quad \hat{p}_{\text{tel}}=v-\hat{p}_N^g,\\
&\text{(IV)}\quad \hat{x}_{\text{tel}}=v-\hat{p}_N^g,\quad \hat{p}_{\text{tel}}=u+\hat{x}_N^g.
\end{aligned} \tag{4}$$

The mapping between $\Pi T(s_k)=T(s_K)T(s_{K-1})\cdots T(s_1)$ and the transformations (I)–(IV) is

$$\begin{aligned}
&\text{(I)}\quad \Leftrightarrow K\equiv 0 \bmod 4,\quad \begin{cases}u=\sum_{k\equiv 3}s_k-\sum_{k\equiv 1}s_k,\\ v=\sum_{k\equiv 0}s_k-\sum_{k\equiv 2}s_k,\end{cases}\\
&\text{(II)}\quad \Leftrightarrow K\equiv 1 \bmod 4,\quad \begin{cases}u=\sum_{k\equiv 1}s_k-\sum_{k\equiv 3}s_k,\\ v=\sum_{k\equiv 0}s_k-\sum_{k\equiv 2}s_k,\end{cases}\\
&\text{(III)}\quad \Leftrightarrow K\equiv 2 \bmod 4,\quad \begin{cases}u=\sum_{k\equiv 1}s_k-\sum_{k\equiv 3}s_k,\\ v=\sum_{k\equiv 2}s_k-\sum_{k\equiv 0}s_k,\end{cases}\\
&\text{(IV)}\quad \Leftrightarrow K\equiv 3 \bmod 4,\quad \begin{cases}u=\sum_{k\equiv 3}s_k-\sum_{k\equiv 1}s_k,\\ v=\sum_{k\equiv 2}s_k-\sum_{k\equiv 0}s_k.\end{cases}
\end{aligned} \tag{5}$$

Since s_k is a linear combination of p_i^g, u and v can also be expressed in the forms of linear combinations of p_i^g:

$$u = \sum_{i=1}^{N-1} \alpha_i p_i^g,$$

$$v = \sum_{i=1}^{N-1} \beta_i p_i^g, \tag{6}$$

where α_i and β_i are coefficients related to c_{ki}. We define the operation set consisting of the four types of transformations in Eq. (4) as universal-variable (UV) transformation (UVT). It is simple to prove the equivalence between UVT and the operations in step (iv) (i.e., the melting operation). In the rest of this paper, we will use these two forms interchangeably.

From Eqs. (3) and (6), $\hat{x}_N^g$, $\hat{p}_N^g$, u, and v can be expressed as

$$\hat{x}_N^g = \hat{R}\begin{pmatrix} I_N \\ 0 \end{pmatrix}, \quad \hat{P}_N^g = \hat{R}\begin{pmatrix} G_N \\ I_N \end{pmatrix}, \tag{7}$$

$$u = \hat{R}\begin{pmatrix} G \\ I \end{pmatrix}\alpha, \quad v = \hat{R}\begin{pmatrix} G \\ I \end{pmatrix}\beta, \tag{8}$$

where

$$\alpha = (\alpha_1 \cdots \alpha_{N-1} \quad 0)^T,$$

$$\beta = (\beta_1 \cdots \beta_{N-1} \quad 0)^T. \tag{9}$$

Generally, $\hat{x}_{\text{tel}}$ and $\hat{p}_{\text{tel}}$ could be any linear combinations of $\hat{x}_i$ and $\hat{p}_i$. With $\hat{x}_{\text{tel}}$ and $\hat{p}_{\text{tel}}$ known, by substituting Eqs. (7) and (8) into Eq. (4), we may solve for α and β. In the senario of teleportation, $\hat{x}_{\text{tel}}$ and $\hat{p}_{\text{tel}}$ should be equal to $(\hat{x}_1, \hat{p}_1)$ when the graph state is perfectly entangled (i.e., all modes except the source mode are infinitely squeezed). Since when $r_i \to \infty$, $\hat{p}_i = e^{-r_i}\hat{p}_i^{(0)} \to 0$, the quadrature variance $\sigma(\hat{p}_i) \to 0$. We allow excess $\hat{p}_i$ for $i=2,\ldots,N$ to emerge in the final state $(\hat{x}_{\text{tel}}, \hat{p}_{\text{tel}})$ but not excess $\hat{x}_i$, which will bring very large excess noise to the final result. Therefore, the final state of mode N should be restricted to the following expression:

$$\hat{x}_{\text{tel}} = \hat{R}\begin{pmatrix} I_1 \\ 0 \\ \forall \end{pmatrix}, \quad \hat{p}_{\text{tel}} = \hat{R}\begin{pmatrix} 0 \\ 1 \\ \forall \end{pmatrix}, \tag{10}$$

where $\forall$ means arbitrary values in the remainder of the column. In the following we demonstrate the calculation process only with the first type of UVT while giving the result for all four types. The calculation of the three remaining types of UVT is similar to that of the first one, except for some exchanges of forms and signs.

For a certain graph G, by substituting Eqs. (7)–(10) into Eq. (4), part (I), with $\hat{R}$ canceled, we obtain equations with α and β as unknown variables:

$$\text{(I)} \quad \begin{pmatrix} I_1 \\ 0 \\ \forall \end{pmatrix} = \begin{pmatrix} G \\ I \end{pmatrix}\alpha + \begin{pmatrix} I_N \\ 0 \end{pmatrix}, \quad \begin{pmatrix} 0 \\ 1 \\ \forall \end{pmatrix} = \begin{pmatrix} G \\ I \end{pmatrix}\beta + \begin{pmatrix} G_N \\ I_N \end{pmatrix}. \tag{11}$$

If the equations have solutions, then mathematically, the graph can be used as a core graph in teleportation via the first type of UVT. After simple calculation, Eq. (11) can be simplified as

$$\text{(I)} \quad G^*\alpha^* = I_1 - I_N, \quad G^*\beta^* = -G_1 - G_N,$$

$$\alpha_1 = 0, \quad \beta_1 = 1, \tag{12}$$

where

$$G^* = (G_2 \cdots G_{N-1}),$$

$$\alpha^* = (\alpha_2 \cdots \alpha_{N-1})^T,$$

$$\beta^* = (\beta_2 \cdots \beta_{N-1})^T. \tag{13}$$

The conditions for equations in Eq. (12) (along with the other three types of UVT) having solutions can be written as

$$\begin{aligned} \text{(I)} \quad \text{rank}(G^*) &= \text{rank}(G^* \quad I_1 - I_N) \\ &= \text{rank}(G^* \quad -G_1 - G_N), \\ \text{(II)} \quad \text{rank}(G^*) &= \text{rank}(G^* \quad -G_1 + I_N) \\ &= \text{rank}(G^* \quad I_1 - G_N), \\ \text{(III)} \quad \text{rank}(G^*) &= \text{rank}(G^* \quad I_1 + I_N) \\ &= \text{rank}(G^* \quad -G_1 + G_N), \\ \text{(IV)} \quad \text{rank}(G^*) &= \text{rank}(G^* \quad -G_1 - I_N) \\ &= \text{rank}(G^* \quad I_1 + G_N). \end{aligned} \tag{14}$$

If any of these equations is satisfied, then graph G can be used as a core graph in teleportation. For instance, if (I) in Eq. (14) stands, then by solving Eq. (12) one can obtain one or more set of α^* and β^*. By using $\alpha=(0\ \alpha^*\ 0)^T$, $\beta=(1\ \beta^*\ 0)^T$, and Eq. (8), one can get the final expressions for u and v. Solving Eq. (12) is more of a linear algebra problem (we employ the pseudoinverse of G^* to solve all these types of equations in this paper). In cases where more than one solution exists, every valid solution is a theoretically possible scheme to implement teleportation. Once the scheme is determined, the final state can be obtained from Eqs. (4), (7), and (8) as

$$\text{(I),(III)} \quad \hat{x}_{\text{tel}} = \hat{x}_1 + \sum_{i=2}^{N-1} \alpha_i \hat{p}_i, \quad \hat{p}_{\text{tel}} = \hat{p}_1 + \sum_{i=2}^{N-1} \beta_i \hat{p}_i \pm \hat{p}_N,$$

$$\text{(II),(IV)} \quad \hat{x}_{\text{tel}} = \hat{x}_1 + \sum_{i=2}^{N-1} \beta_i \hat{p}_i \pm \hat{p}_N, \quad \hat{p}_{\text{tel}} = \hat{p}_1 + \sum_{i=2}^{N-1} \alpha_i \hat{p}_i, \tag{15}$$

which has the noise expression

$$\text{(I),(III)} \quad \sigma(\hat{x}_{\text{tel}}) = \sigma(\hat{x}_1) + \sum_{i=2}^{N-1} \alpha_i^2 e^{-2r_i},$$

$$\sigma(\hat{p}_{\text{tel}}) = \sigma(\hat{p}_1) + \sum_{i=2}^{N-1} \beta_i^2 e^{-2r_i} + e^{-2r_N},$$

$$\text{(II),(IV)} \quad \sigma(\hat{x}_{\text{tel}}) = \sigma(\hat{x}_1) + \sum_{i=2}^{N-1} \beta_i^2 e^{-2r_i} + e^{-2r_N},$$

$$\sigma(\hat{p}_{\text{tel}}) = \sigma(\hat{p}_1) + \sum_{i=2}^{N-1} \alpha_i^2 e^{-2r_i}, \tag{16}$$

with vacuum variance normalized to unity. Note that generally, for a certain graph state, $\sigma(\hat{x}_{\text{tel}})$ and $\sigma(\hat{p}_{\text{tel}})$ are not equal.

When the source mode is in a Gaussian state, the fidelity of teleportation $F \equiv \langle \alpha_1 | \hat{\rho}_{\text{tel}} | \alpha_1 \rangle$ can be derived as

$$F = \frac{2}{\sqrt{[\sigma(\hat{x}_1) + \sigma(\hat{x}_{\text{tel}})][\sigma(\hat{p}_1) + \sigma(\hat{p}_{\text{tel}})]}}. \tag{17}$$

For infinite squeezing, $\sigma(\hat{x}_{\text{tel}})$ in Eq. (16) becomes $\sigma(\hat{x}_1)$, while $\sigma(\hat{p}_{\text{tel}})$ becomes $\sigma(\hat{p}_1)$. Therefore $F=[\sigma(\hat{x}_1)\sigma(\hat{p}_1)]^{-1}$, which equals 1 for coherent and squeezed states. Any finite r_i for $i=2,\ldots,N$ will reduce F to less than unity. Reducing the excess noise of either quadrature could lead to a better fidelity.

C. Some remarks

Now we explain the theoretical necessity of step (i) in the protocol. Suppose G is a three-mode graph state with every mode connected with the remaining two modes, i.e.

$$G = \begin{pmatrix} 0 & 1 & 1 \\ 1 & 0 & 1 \\ 1 & 1 & 0 \end{pmatrix}$$

[see Fig. 1(e)]. It is easy to verify that no equation in Eq. (14) is satisfied. So G could not be used as a core graph in teleportation. However, it is obvious that teleportation via the subgraph consisting of modes 1 and 3 (i.e., the source and target modes) can be implemented by performing $T(p_1^g)$. Although it can hardly be called teleportation, in which the source mode and the target mode are coupled directly, the essence is still the same. Actually, it is the prototype of cluster-state quantum computation [7] with the operator $D=I$. Such a subgraph can be disconnected from the original tripartite entanglement by step (i). Furthermore, under our protocol, when the gain of QND interaction is unity, as long as the source and target modes are connected (directly or indirectly), there is at least one teleportation scheme with

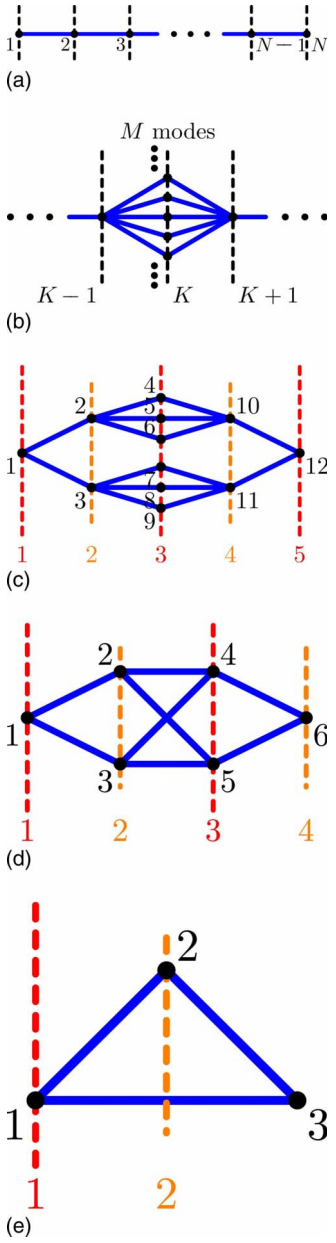

FIG. 1. (Color online) (a) Linear graph state of N modes. Numbers denote the indices of modes, and also their corresponding levels. Dashed lines visualize each level. (b) Multiple-rail optimization on the Kth level. (c) A generalization of the multiple-rail model, with branches at both even and odd levels. (d) A further optimized scheme using the multiple-rail model. (e) A simple graph which cannot be used as a core graph due to parity contradiction on mode 3's level.

disconnection operation allowed—disconnection of a linear path from the source to the target mode. In the next section we will see that any one-dimensional graph state with unit g could be used as a core graph.

As we will prove in the next section, our protocol often obtains better fidelity in teleportation via two- and multidimensional graph states than does linear teleportation. The essential reason for its advantage compared to linear teleportation lies in the nonequivalence between the two kinds of distillation. Only the melting operation may increase the

quality of entanglement in distillation of multidimensional graph states. The concept of the protocol is to try to make the best use of the melting operation to obtain better (maybe the best) entanglement, which leads to higher fidelity in teleportation. A core graph is a typical subgraph on which the whole distillation process can be done with only the melting operation.

III. TELEPORTATION VIA TYPICAL GRAPH STATES

In the last section we discussed generally whether an arbitrary graph state G could be used as a core graph in teleportation. In this section, we will investigate several important properties of some typical core graph types in more detail. Since the fidelity F can be completely determined by the excess noise of both quadratures when the source mode is certain, we will mainly focus on more details of the excess noise of each quadrature in the following discussion. Using this approach, we may find some conclusions very easy to interpret. Also, to simplify the discussion, in this and the next section we will focus on graph states on which the QND interaction is implemented with a gain of unity (i.e., $g_{ij}=1$).

A. Linear graph states

Consider a one-dimensional graph state consisting of N modes [Fig. 1(a)]. After $T(p_1^g)T(p_2^g)\cdots T(p_{N-1}^g)$, mode N is rectified to

$$\hat{x}_{\mathrm{tel}} = \hat{x}_1 + \sum_{k=1}^{\lfloor N/2 \rfloor} (-1)^{k+1} \hat{p}_{2k},$$

$$\hat{p}_{\mathrm{tel}} = \hat{p}_1 + \sum_{k=1}^{\lfloor (N-1)/2 \rfloor} (-1)^{k} \hat{p}_{2k+1}, \tag{18}$$

with total noise

$$\sigma(\hat{x}_{\mathrm{tel}}) = \sigma(\hat{x}_1) + \sum_{k=1}^{\lfloor N/2 \rfloor} e^{-2r_{2k}},$$

$$\sigma(\hat{p}_{\mathrm{tel}}) = \sigma(\hat{p}_1) + \sum_{k=1}^{\lfloor (N-1)/2 \rfloor} e^{-2r_{2k+1}}, \tag{19}$$

where $\lfloor \cdot \rfloor$ is the floor operator. Therefore, any linear graph state with unit gain of the QND interaction can be used as a core graph. From Eq. (19) we see that the excess noise of different quadratures is affected by different modes. Defining level l_i which denotes the number of steps from the first (source) mode to the ith mode plus 1 (so that the source mode is at level 1), $\sigma(\hat{x}_{\mathrm{tel}}-\hat{x}_1)$ is affected by the modes at even levels, while $\sigma(\hat{p}_{\mathrm{tel}}-\hat{p}_1)$ is affected by the modes at odd levels. If in some cases we mainly care about one of the quadratures while the other can be largely ignored, then the graph state can be prepared in a cheaper way by squeezing every corresponding-level mode while leaving the other unsqueezed. Compared with the usual scheme where all modes are squeezed, the excess noise of the quadrature we are concerned with is intact, while that of the other quadrature grows very large, with the benefit of reduced cost. Another obvious yet important conclusion is that addition of one mode at the end of the serial graph (i.e., increase in the total level) increases either $\sigma(\hat{x}_{\mathrm{tel}})$ or $\sigma(\hat{p}_{\mathrm{tel}})$, thus decreasing the teleportation fidelity.

B. Multiple-rail model

Let us modify the Kth level of the linear graph in [Fig. 1(a)] to a multiple-rail configuration [9] [Fig. 1(b)] with M modes, respectively, with index $(K,1)$, $(K,2),\ldots,(K,M)$, each coupling with the modes at the $(K-1)$th and the $(K+1)$th levels. After $T(p_1^g)\cdots T(p_{K-1}^g)T[(\Sigma_M p_{K,i}^g)/M]T(p_{K+1}^g)\cdots T(p_{N-1}^g)$, $\hat{p}_K$ in Eq. (18) is replaced by $(1/M)\Sigma_M \hat{p}_{K,i}$, which has a variance $(1/M^2)\Sigma_M e^{-2r_{K,i}}$. If all r's are set equal, the variance is equal to $(1/M)e^{-2r}$, equivalent to that of a single mode which has a squeezing degree of $r'=r+\frac{1}{2}\ln M$. When $M\to\infty$, the equivalent $r'\to\infty$, and the fidelity of teleportation will not be negatively affected by the modes in the Kth level. Note that if K is even (including 2, in which case the source mode is coupled directly with M modes), the excess noise of $\hat{x}_{\mathrm{tel}}$ can be reduced, or $\hat{p}_{\mathrm{tel}}$ can be more accurately obtained in the other case. If this model is used on both the even and the odd levels of the graph, it is quite straightforward to deduce that both $\sigma(\hat{x}_{\mathrm{tel}})$ and $\sigma(\hat{p}_{\mathrm{tel}})$ can be alleviated. Such multiple rails can improve the teleportation quality and thus compensate the limited r. Aside from the first (source) and the last (target) level, any level in between can be multiplied to several rails and thus reduce the excess noise in teleportation. We have shown that unbalanced excess noise can be used in cases where precision is not equally required in $\hat{x}$ and $\hat{p}$. For different precision standards, we can choose different numbers of rails (i.e., the costs of constructing the graph states) to reach an optimized trade-off between cost and precision.

Using the concept of multiple rails, more sophisticated graphs with better teleportation quality can be utilized in higher-precision-demanding tasks. By simply branching from both the even and the odd levels, we can construct graphs like that shown in Fig. 1(c). After performing the first type of UVT with $u=\frac{1}{2}(p_2^g+p_3^g)-\frac{1}{2}(p_{10}^g+p_{11}^g)$, $v=p_1^g-\frac{1}{3}(p_4^g+p_5^g+p_6^g)-\frac{1}{3}(p_7^g+p_8^g+p_9^g)$, mode 12 is transformed into $\hat{x}_{\mathrm{tel}}=\hat{x}_1+\frac{1}{2}(\hat{p}_2+\hat{p}_3)-\frac{1}{2}(\hat{p}_{10}+\hat{p}_{11})$, $\hat{p}_{\mathrm{tel}}=\hat{p}_1-\frac{1}{3}(\hat{p}_4+\hat{p}_5+\hat{p}_6)-\frac{1}{3}(\hat{p}_7+\hat{p}_8+\hat{p}_9)+\hat{p}_{12}$. The excess noise in both $\hat{x}$ and $\hat{p}$ is reduced in comparison with linear five-mode graph-state teleportation (again, assuming the r's are equal). However, the factor $1/2$ produced by branching from mode 1 is applied only on the even levels (i.e., on modes 2, 3, 10, and 11), while not on the odd levels (i.e., on modes 4, 5, 6, 7, 8, and 9), and the total factor affected on the odd levels is $1/3$, not $1/6$. Therefore, the lower branch, which consists of modes 3, 7, 8, 9, and 11, actually increases the excess noise of $\hat{p}$ while reducing the excess noise of $\hat{x}$. A further optimized scheme using the multiple-rail model is shown in Fig. 1(d). In this graph state, no mode has a negative effect in controlling the excess noise of either quadrature. After the fourth type of UVT where $u=\hat{p}_1^g-\frac{1}{2}(\hat{p}_4^g+\hat{p}_5^g)$ and $v=\frac{1}{2}(\hat{p}_2^g+\hat{p}_3^g)$, mode 6 is transformed into $\hat{x}_{\mathrm{tel}}=\hat{x}_1+\frac{1}{2}(\hat{p}_2+\hat{p}_3)-\hat{p}_6$ and $\hat{p}_{\mathrm{tel}}=\hat{p}_1-\frac{1}{2}(\hat{p}_4+\hat{p}_5)$. However, to see it in the level perspective, all these graphs can still be

seen as a series of levels, just like the one-dimensional graph. The excess noise still follows the same rule that different quadratures are affected by modes at levels of different parity. This view gives us another approach to quickly determine graph like Fig. 1(e) cannot be used as a core graph since with the existence of mode 2, parity of mode 3's level cannot be determined. Thus, the investigation of the teleportation property of a bipartite graph (also known as a two-colorable graph) may be particularly worthwhile in the future.

In general, if the squeezing degree is fixed, to reach a higher fidelity in teleportation, two main approaches can be considered. One is to shorten the overall length (i.e., the total number of levels) of the entanglement network. The other is to use more multiple rails to diminish every mode's contribution to the excess noise.

IV. APPLICATION: TELEPORTATION VIA TWO-DIMENSIONAL CLUSTER STATES

The discussion above is mainly focused on the property of a graph being used as a core graph. However, in practical situations, the entanglement network prepared before teleportation may be a very large and sophisticated graph which can support concurrent teleportation tasks or simply cannot be used as a core graph. In such cases, disconnection of suitable subgraphs is necessary and should be done with careful planning.

Consider an arbitrary square lattice cluster state. Teleportation via such a typical entanglement state may be frequently used in the future. In the following discussion, to be consistent with the understanding that the cluster state is independently prepared before coupling with the source mode, we name the source mode 0 and let the indices of the modes in the cluster state begin from 1. First we show that generally square lattice cluster states bring less excess noise in teleportation than do linear graph states, keeping both r and g fixed. For the simplicity of our discussion, again, we assume that r for all the modes (except the source mode) are same. Consider designing an $(M\times N)$-partite entanglement network to support teleportation between two arbitrary parties. A simple scheme is to build a linear (could be a loop) graph state contains all parties. However, the furthest distance from two parties is at least $\frac{1}{2}M\times N$ steps, which means the final excess noise may contain variances of $\mathcal{O}(M\times N)$ modes. A square lattice cluster state could remarkably reduce the excess noise from the environment—$\mathcal{O}(M+N)$ steps is required to teleport from one mode to another. Further, in each step, excess noise can be alleviated even more because of the multiple-rail optimization.

First let us consider an $N\times N$ rather than an $M\times N$ lattice. Later we will see that the teleportation scheme for such a state can be easily generalized to that on an $M\times N$ lattice. Assuming that station 1 wants to teleport its quantum information on mode 0 to station N^2. In the case of $N=2$ [see Fig. 2(a)], after the fourth type of UVT with $u=p_0^g-\frac{1}{2}(p_2^g+p_3^g)$, $v=p_1^g$, mode 4 becomes $\hat{x}_{\text{tel}}=\hat{x}_0+\hat{p}_1-\hat{p}_4$, $\hat{p}_{\text{tel}}=\hat{p}_0-\frac{1}{2}(\hat{p}_2+\hat{p}_3)$ with excess noise $\sigma(\hat{x}_{\text{tel}}-\hat{x}_0)=e^{-2r_1}+e^{-2r_4}$, $\sigma(\hat{p}_{\text{tel}}-\hat{p}_0)=\frac{1}{4}(e^{-2r_2}+e^{-2r_3})$, with $\sigma(\hat{p}_{\text{tel}}-\hat{p}_0)$ better than that in a linear scheme. When $N=3$ [see Fig. 2(b)], similar results can be shown that after the second type of UVT with $u=p_0^g-\frac{1}{2}(p_2^g+p_3^g)+\frac{1}{2}(p_7^g+p_8^g)$, $v=p_1^g-\frac{1}{3}(p_4^g+2p_5^g+p_6^g)$, the final state becomes $\hat{x}_{\text{tel}}=\hat{x}_0+\hat{p}_1-\frac{1}{3}(\hat{p}_4+2\hat{p}_5+\hat{p}_6)+\hat{p}_9$, $\hat{p}_{\text{tel}}=\hat{p}_0-\frac{1}{2}(\hat{p}_2+\hat{p}_3)$

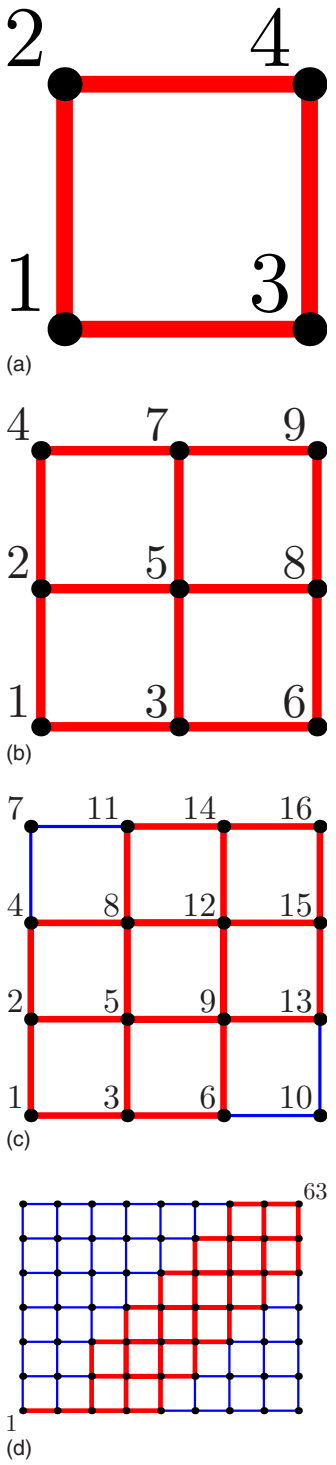

FIG. 2. (Color online) $M\times N$ cluster-state teleportation network. The coupling of the source mode 0 with mode 1 is not drawn here. (a) 2×2 cluster state. (b) 3×3 cluster state. (c) 4×4 cluster state. Red (bold) part is one of the valid simplest core graphs. (d) 7×9 cluster state with one of its simplest core graphs drawn in red (bold).

$+\frac{1}{2}(\hat{p}_7+\hat{p}_8)$, with excess noise $\sigma(\hat{x}_{\text{tel}}-\hat{x}_0)=e^{-2r_1}+\frac{1}{9}(e^{-2r_4}+4e^{-2r_5}+e^{-2r_6})+e^{-2r_9}$, $\sigma(\hat{p}_{\text{tel}}-\hat{p}_0)=\frac{1}{4}(e^{-2r_2}+e^{-2r_3})+\frac{1}{4}(e^{-2r_7}+e^{-2r_8})$, both better than that in a linear teleportation. However, when $N=4$ [see Fig. 2(c)], one solution is the fourth type of UVT with $u=p_0^g-\frac{1}{2}(p_2^g+p_3^g)+\frac{1}{2}(p_8^g+p_9^g)-\frac{1}{2}(p_{14}^g+p_{15}^g)$, $v=p_1^g-\frac{1}{3}(p_4^g+2p_5^g+p_6^g)+\frac{1}{3}(p_{11}^g+2p_{12}^g+p_{13}^g)$. We see that not all modes need to be measured (such as modes 7 and 10)—they can be measured, but the results will not be used in either u or v, therefore they can be simply discarded. Note that, although modes 7 and 10 are useless, they still can be in an effective core graph—unlike mode 2 in Fig. 1(e) which has to be disconnected so that teleportation from mode 1 to mode 3 is feasible, the existence of modes 7 and 10 in Fig. 2(c) does not harm the graph's ability to teleport, so they can just as well remain in the core graph. Similarly, when $N>4$, not all the entanglement resources need to be destroyed during teleportation. After discarding all the useless modes in a core graph, we get the simplest core graph with equivalent teleportation ability. In random source-target teleportation, this may lead to a saving of more resources, while in fixed source-target scenario, cheaper (with fewer modes and QND interactions) entanglement networks can be designed as the simplest core graphs.

Now we generalize the cluster states to arbitrary $M\times N$ lattices. Assuming $M\geqslant N$, a simple way to implement teleportation via such states is to first select an $N\times N$ subgraph in it and then draw two shortest paths to connect the subgraph to the source and the target modes, respectively. The overall teleportation quality is better than that of a one-dimensional one. A scheme for teleportation on a 7×9 cluster state is shown in Fig. 2(d).

V. A UNIVERSAL WAY TO DISTILL GRAPH-STATE ENTANGLEMENT NETWORKS

The essence of graph-state teleportation is to distill the whole graph state to a direct source-target bipartite entanglement. The only difference between teleportation and distillation is that teleportation requires one to measure the source mode and perform the corresponding operation $T(s_{\text{src}})=T(c_{\text{src}}p_{\text{src}}^g)$ described in step (iv) of the protocol, while distillation does not. Thus, teleportation via a graph state is essentially the same as distillation of the graph state to a bipartite entanglement containing both the source and target modes. As mentioned before, step (i) corresponds to the first type of distillation operation—disconnection—while steps (iii) and (iv) (i.e., UVT) correspond to the melting operation which creates new entanglement in the process of destroying the old ones. Therefore, a graph state can be distilled to a bipartite entanglement between two particular modes using only the melting operation if it can be used as a core graph in teleportation between these two modes. Otherwise, a disconnection operation is required to assist the distillation.

It is easy to find a way to distill a certain graph state according to the factors determined in the UVT—one intuitive way is to change the form of the operation from a UVT to that of $T(s_{\text{src}})\Pi_{\text{other}}T(s_k)$ and then omit $T(s_{\text{src}})$ which takes the measurement result of $\hat{p}_{\text{src}}$ as parameter. After $\Pi_{\text{other}}T(s_k)$, the graph state is successfully distilled to a bipartite entanglement. A further $T(s_{\text{src}})$ will have the source mode teleported to the target. Since teleportation via multidimensional graph states may have better quality than that via one-dimensional graph states, it is straightforward to conclude that the bipartite entanglement distilled from multidimensional graph states may be better than that distilled from one-dimensional graph states.

For instance, consider the graph state in Fig. 1(b) with $K=2$ and three total levels. Assuming all g's are equal and $r_{2,i}=r$ for $i=1,2,\ldots,M$. As discussed in Sec. III B, teleportation from mode 1 to mode 3 can be implemented by performing $T(p_1^g)T((\Sigma_M p_{2,i}^g)/gM)$ on mode 3, and the excess noise is $\sigma(\hat{x}_{\text{tel}}-\hat{x}_1)=(1/g^2M)e^{-2r}$, $\sigma(\hat{p}_{\text{tel}}-\hat{p}_1)=\sigma(\hat{p}_3)$. When

$$g^2Me^{2r}\to\infty, \tag{20}$$

modes in level 2 will not bring excess noise into the final state—the multiple rails are equivalent to a single rail which contains a mode with $r'=\ln g+\frac{1}{2}\ln M+r\to\infty$. Translating to the language of entanglement distillation, if modes 1 and 3 are perfectly squeezed and Eq. (20) is satisfied, after performing $T((\Sigma_M p_{2,i}^g)/gM)$ on mode 3, the graph state can be perfectly distilled to a two-mode entanglement between modes 1 and 3. Note that at some level Eq. (20) shows internal conversion among M, g, and r—they compensate each other by their different strengths. When M is very large, even in the case where QND interaction is very weak ($g\ll 1$) or the squeezing factor r of the modes in level 2 is very small, the graph state can still be distilled to very good bipartite entanglement. Here a significant discontinuity emerges—in the limit of infinite squeezing (i.e., $r\to\infty$), the value of the left expression in Eq. (20) leaps from 0 to ∞ when g changes from zero to nonzero. This effect reveals the essential role QND coupling plays in creating entanglement—mathematically speaking, perfect entanglement can be created once the modes are coupled—it is not a matter of time. In that case, the quality of the distilled entanglement will not depend on the graph G, just as indicated in Eq. (16), where all terms with coefficients α and β vanish.

VI. CONCLUSION

In this paper, we investigated the feasibility of continuous-variable quantum teleportation via one- and higher-dimensional graph states under the protocol constituted by the entanglement disconnection operation and $F^{\dagger}X(-s)$ transformation (or an equivalent UV transformation). The exact method can be calculated according to a systematic approach, with the final state and the teleportation fidelity (or the excess noise for each quadrature) being obtained. The adjacency matrix G plays a significant role here. By examining the properties of several kinds of graph states, we find two features of graph-state teleportation that are useful in controlling the excess noise of the final state. One is that the excess noise of $\hat{x}$ and $\hat{p}$ is affected by different levels of the teleportation network. This effect enables us to lower our cost of squeezing the modes which affect the quadrature of little interest in certain encoding operations, while not affecting the other quadrature that we need. The other property is the noise-reduction ability in the multiple-rail model,

which may compensate the imperfect entanglement due to finite squeezing. As an application of our method and also a demonstration of the last two properties of graph-state teleportation, we brought forward a simple solution for $M \times N$-partition cluster-state teleportation with better excess noise control compared with linear teleportation, which may become usefull in future. Further, in fixed source-target scenarios, our scheme can be simplified to a cheaper yet equivalent one (i.e., preparation of only the simplest core graph) which may be particularly useful in a quantum repeater.

Based on the conclusion we drew on teleportation, a universal way to distill bipartite entanglement from a graph state is obtained, with (possibly) better quality of the bipartite entanglement comparing with the one-dimensional melting scheme. In addition, teleportation on graph states prepared with nonunit gain of the QND interaction g is briefly discussed, with observation of the discontinuity of the fidelity in the limit of infinite squeezing when g changes from zero to nonzero. Taking cost into consideration, the times of QND interaction (i.e., M, the number of rails), the gains of QND interaction, g, and the single-mode squeezing degree r can be essentially converted into each other. One may choose different combinations of M, g, and r according to the variance of cost of each kind of resource and the required upper bound of the excess noise of the final state.

It is also worthwhile to mention that the mathematical model employed in this paper helps one to find one or more sets of solutions for teleportation via arbitrary graph states, yet it cannot automatically give the best (i.e., the cheapest, the lowest excess noise, etc.) solution. In addition, using this model, the design of graph G for a certain purpose [i.e., replace the vector in Eq. (10) with certain expression, to perform operations other than teleportation] is also possible. More investigations are needed to exploit the full potential of graph-state "teleoperation" (remote implementaton of operations).

ACKNOWLEDGMENTS

This work was supported by the National Natural Science Foundation of China (Grant No. 60773085), Shanghai Jiao Tong University (SJTU) Young Teacher Foundation (Grant No. A2831B), and SJTU PRP (Grant No. T03013002).

[1] C. H. Bennett, G. Brassard, C. Crepeau, R. Jozsa, A. Peres, and W. K. Wootters, Phys. Rev. Lett. **70**, 1895 (1993).
[2] S. L. Braunstein and H. J. Kimble, Phys. Rev. Lett. **80**, 869 (1998).
[3] L. Vaidman, Phys. Rev. A **49**, 1473 (1994).
[4] S. L. Braunstein, C. A. Fuchs, and H. J. Kimble, J. Mod. Opt. **47**, 267 (2000).
[5] P. Grangier and F. Grosshans, e-print arXiv:quant-ph/0009079v1.
[6] P. van Loock and S. L. Braunstein, Phys. Rev. Lett. **84**, 3482 (2000).
[7] N. C. Menicucci, P. van Loock, M. Gu, C. Weedbrook, T. C. Ralph, and M. A. Nielsen, Phys. Rev. Lett. **97**, 110501 (2006).
[8] J. Zhang and S. L. Braunstein, Phys. Rev. A **73**, 032318 (2006).
[9] P. van Loock, C. Weedbrook, and M. Gu, Phys. Rev. A **76**, 032321 (2007).